

## Heterodyne Measurements of Hot Bands and Isotopic Transitions of N<sub>2</sub>O Near 7.8 μm

**A. Hinz**

Institut für Angewandte Physik der Universität Bonn, Bonn,  
Federal Republic of Germany

**J.S. Wells**

Time and Frequency Division, National Bureau of Standards, Boulder, Colorado, USA

**A.G. Maki**

Molecular Spectroscopy Division, National Bureau of Standards, Gaithersburg,  
Maryland, USA

Received December 9, 1986

Heterodyne frequency measurements are reported for absorption transitions of N<sub>2</sub>O in the frequency range from 1257 to 1335 cm<sup>-1</sup>. The measurements use a CO laser as a transfer oscillator whose frequency is measured directly against combinations of frequencies of two stabilized CO<sub>2</sub> lasers whose frequencies are well known. A tunable diode laser is locked to the N<sub>2</sub>O absorption feature and the frequency difference is measured between the diode laser and the CO laser. The ν<sub>3</sub> fundamental bands of the <sup>15</sup>N<sup>14</sup>N<sup>16</sup>O and <sup>14</sup>N<sup>15</sup>N<sup>16</sup>O isotopes are reported. Measurements are also given for the 00<sup>0</sup>2–00<sup>0</sup>1, 02<sup>0</sup>1–02<sup>0</sup>0, and 02<sup>2</sup>1–02<sup>2</sup>0 vibrational transitions of N<sub>2</sub>O. A table of frequencies is given for the 00<sup>0</sup>2–00<sup>0</sup>0 band near 2560 cm<sup>-1</sup> based on these and earlier measurements.

PACS: 33.20Ea; 35.20Pa; 35.80+s

### Introduction

In three earlier papers [1–3], we presented heterodyne measurements on infrared transitions of nitrous oxide (N<sub>2</sub>O) that can be used to tie the frequencies of infrared transitions to the cesium frequency standard in order to provide accurate frequency benchmarks for the calibration of infrared frequency measurements. The present heterodyne measurements supplement those earlier papers by presenting frequency measurements on the weaker hot band features of the ν<sub>3</sub> band<sup>1</sup>

<sup>1</sup> The vibrational numbering system adopted by the IAU-IUPAP joint commission of spectroscopy [4] is used throughout this paper, as we have also done in [3]. Most other authors use a notation that interchanges ν<sub>1</sub> and ν<sub>3</sub>

near 1280 cm<sup>-1</sup>. Such hot band features by themselves can be used to provide a denser comb of calibration standards, but we believe they are most useful because they can be combined with other data to provide absolute frequency data for other frequency regions such as the 00<sup>0</sup>2–00<sup>0</sup>0 band near 2560 cm<sup>-1</sup>, or the 02<sup>0</sup>1–00<sup>0</sup>0 band near 2460 cm<sup>-1</sup>.

Although the present measurements and those of Refs. [1–3, 5] are the only true frequency measurements of vibrational levels of N<sub>2</sub>O, there are a number of very good wavelength measurements on the same levels of N<sub>2</sub>O [6–10] and frequency measurements of rotational transitions involving the same vibrational states [11]. The present measurements were analyzed with the aid of those earlier measurements in

**Table 1.** Heterodyne frequency measurements on various bands<sup>a</sup> of nitrous Oxide near 1280 cm<sup>-1</sup>

Transfer oscillator		Nitrous oxide		Obs.-calc.	
CO trans. $P_v(J'')$	Synthesized freq. <sup>b</sup> MHz	N <sub>2</sub> O trans.	Measured freq. <sup>c</sup> MHz	Freq. MHz	
		Rot.	Band		
$P_{34}(8)$	37872657.9	$P(34)$	$S$	37874751.3(20)	0.1
$P_{33}(10)$	38408472.3	$P(15)$	$S$	38400350.6(20)	-0.3
$P_{33}(8)$	38587420.9	$P(8)$	$S$	38584684.3(20)	-0.6
$P_{32}(13)$	38842887.6	$R(1)$	$S$	38839105.2(40)	2.8
$P_{31}(6)$	39263198.2	$R(19)$	$S$	39270101.8(60)	1.2
$P_{31}(9)$	39928620.4	$R(50)$	$S$	39929466.5(100)	-0.3
$P_{33}(12)$	38225471.6	$P(25)^e$	$T^d$	38226482.9(30)	0.6
$P_{33}(12)$	38225471.6	$P(25)^f$	$T$	38226668.5(30)	0.1
$P_{33}(9)$	38498453.1	$P(15)$	$T$	38496873.0(30)	-0.6
$P_{32}(11)$	39029957.2	$R(5)$	$T$	39033831.1(60)	0.8
$P_{31}(10)$	39836563.0	$R(40)^e$	$T$	39834054.1(70)	-4.7
$P_{31}(10)$	39836563.0	$R(40)^f$	$T$	39834244.5(70)	0.3
$P_{31}(8)$	40019664.8	$R(49)^e$	$T$	40020283.8(60)	1.8
$P_{31}(8)$	40019664.8	$R(49)^f$	$T$	40020875.4(60)	0.1
$P_{34}(10)$	37695777.7	$P(24)$	$U$	37699186.0(20)	-0.4
$P_{33}(12)$	38225471.6	$P(4)$	$U$	38225885.4(20)	-0.4
$P_{33}(10)$	38408472.3	$R(2)$	$U$	38401010.9(20)	1.1
$P_{33}(9)$	38498453.1	$R(6)$	$U$	38498898.3(30)	-1.6
$P_{32}(13)$	38842887.6	$R(21)$	$U$	38851769.4(20)	0.3
$P_{32}(11)$	39029957.2	$R(29)$	$U$	39030777.7(60)	1.6
$P_{31}(16)$	39263198.2	$R(40)$	$U$	39266556.4(90) <sup>g</sup>	-1.6
$P_{31}(10)$	39836563.0	$R(69)$	$U$	39833272.8(80)	0.0
$P_{31}(8)$	40019664.8	$R(49)^f$	$V^d$	40017155.4(100)	<sup>h</sup>
$P_{31}(8)$	40019664.8	$R(50)^e$	$V$	40022468.7(105) <sup>g</sup>	<sup>h</sup>
$P_{33}(10)$	38408472.3	$P(23)$	$W$	38404371.3(20)	<sup>h</sup>
$P_{31}(8)$	40019664.8	$R(43)$	$W$	40022207.0(60)	<sup>h</sup>
$P_{34}(10)$	37695777.7	$P(26)$	$I$	37695138.6(20)	0.4
$P_{33}(10)$	38408472.3	$R(0)$	$I$	38409060.2(40) <sup>g</sup>	-0.5
$P_{32}(13)$	38842887.6	$R(18)$	$I$	38840091.7(20)	0.1
$P_{31}(14)$	39458296.3	$R(47)$	$I$	39456943.8(80)	-6.1
$P_{34}(10)$	37695777.7	$P(15)$	$J$	37696318.9(20)	0.4
$P_{34}(8)$	37872657.9	$P(8)$	$J$	37873541.4(20)	-0.8
$P_{32}(13)$	38842887.6	$R(33)$	$J$	38838294.4(40)	1.7

<sup>a</sup> The notation for the <sup>14</sup>N<sub>2</sub><sup>16</sup>O bands is as follows:  $S \equiv 02^01-02^00$ ,  $T \equiv 02^21-02^20$ ,  $U \equiv 00^02-00^01$ ,  $V \equiv 03^11-03^10$ , and  $W \equiv 03^31-03^30$ .  $I$  and  $J$  refer to the  $10^00-00^00$  bands of <sup>14</sup>N<sup>15</sup>N<sup>16</sup>O and <sup>15</sup>N<sup>14</sup>N<sup>16</sup>O, respectively

<sup>b</sup> We estimate the synthesis frequency is accurate to  $\pm 0.2$  MHz and that it represents the center of the CO transition to  $\pm 3.0$  MHz

<sup>c</sup> The uncertainty in the last digits is given in parentheses

<sup>d</sup> The <sup>e</sup> and <sup>f</sup> given after some rotational quantum numbers refer to the parity of the doublet levels (see [23])

<sup>g</sup> Average uncertainties; actual values for these measurements were (-60,120), (-150,60), and (-20,60)

<sup>h</sup> No attempt was made to fit these measurements due to insufficient data from these experiments and other sources

order to provide an accurate set of ro-vibrational constants and an appropriate variance-covariance matrix which are being used to provide tables of calibration frequency standards and their estimated uncertainties.

## Experimental Technique

Table 1 presents the results of the present frequency measurements. Each of the measurements in Table 1 is a combination of two nearly simultaneous measurements. One measurement consists of a determination

of the frequency of a CO laser relative to stabilized CO<sub>2</sub> laser frequency standards. The second measurement is a difference frequency between the CO laser and a tunable diode laser (TDL) whose frequency is locked to the N<sub>2</sub>O absorption feature of interest. The frequency measurements are algebraically combined to give the frequency for the N<sub>2</sub>O transition. The CO laser functions as a transfer oscillator in this scheme. There are two reasons for this procedure. First, we have not been able to use the TDL with the Metal-Insulator-Metal (MIM) diode in a direct synthesis experiment, and thus we require the transfer oscillator.

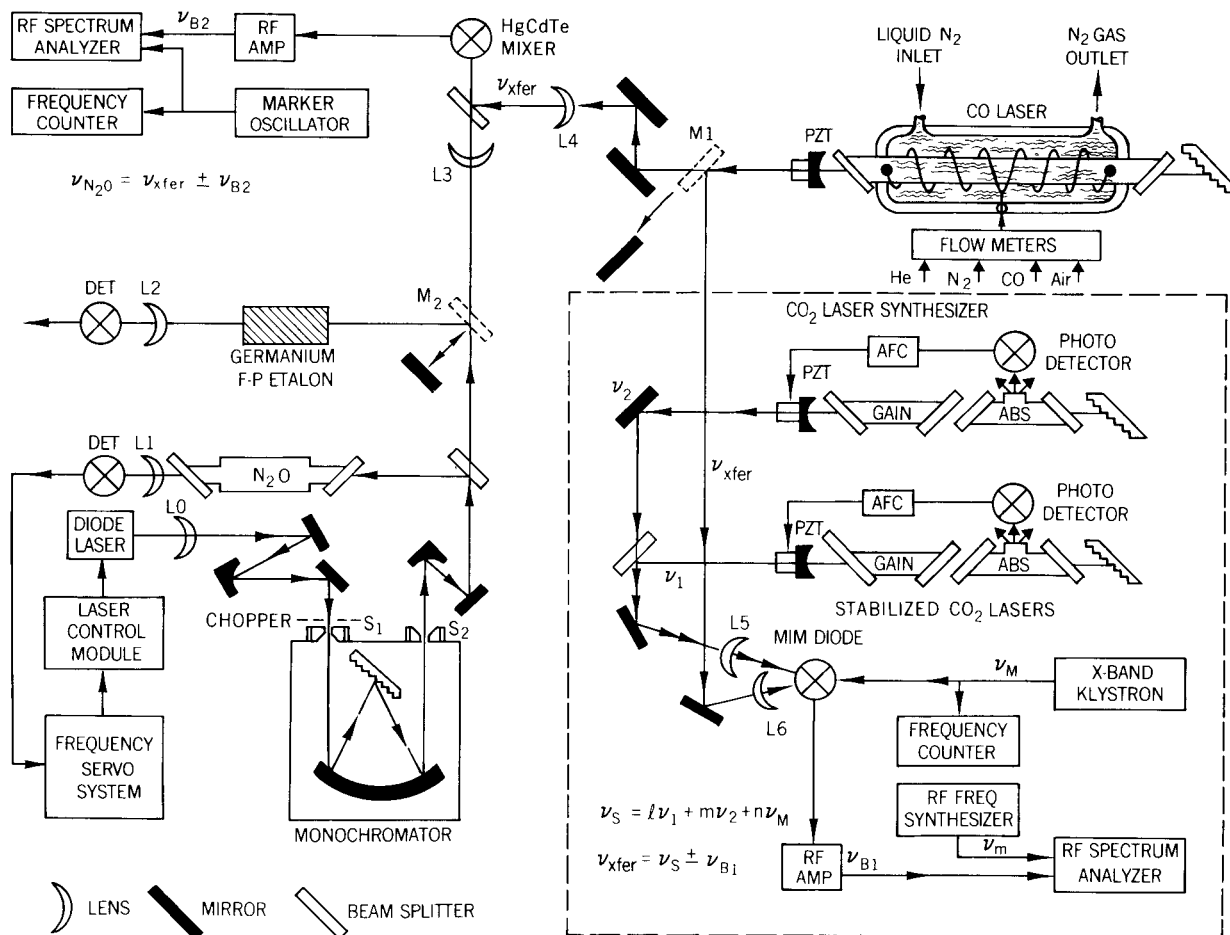


Fig. 1. Block diagram of heterodyne frequency measurement system is shown with the kinematically mounted mirrors,  $M_1$  and  $M_2$ , in the appropriate positions for the heterodyne measurement of  $\nu_{B2}$ . The gas mixture for the CO laser is cooled by flowing the gas through glass coils immersed in liquid nitrogen before it enters the laser tube at both ends, just inside the end electrodes (the three electrodes are not shown). The mixture is exhausted at mid-bore through the center electrode. The symbols for the beat note equations are indicated in the text

Second, the CO frequencies in the literature [12, 13] disagreed with our measured CO values by more than our desired objective of a  $\pm 3$  MHz uncertainty in the  $N_2O$  measurement.

A block diagram of the measurement system is shown in Fig. 1. The three functional groupings consisted of 1) a  $CO_2$  laser frequency synthesizer, 2) a tunable diode laser assembly, and 3) the CO laser transfer oscillator. The  $CO_2$  laser synthesizer was composed of the components at the bottom and on the right hand side of the figure. They consisted of two stabilized  $CO_2$  lasers, a phase-locked microwave oscillator and frequency counter, a MIM diode, and a combination of an RF amplifier, RF spectrum analyzer, and a 0 to 1.0 GHz frequency synthesizer. When radiation from the two  $CO_2$  lasers and the microwave oscillator was coupled to the diode, currents were generated in the MIM diode at a synthesized frequency,

$\nu_s$ , given by:

$$\nu_s = l\nu_1 + m\nu_2 + n\nu_M, \tag{1}$$

where  $\nu_1$  and  $\nu_2$  were the frequencies of the  $CO_2$  laser frequency standards, and  $\nu_M$  is a microwave frequency. The quantities  $l$ ,  $m$ , and  $n$  are integers which are allowed both positive and negative values. The quantity  $[1 + |l| + |m| + |n|]$  is called the mixing order; both sixth and seventh order mixing were required for these measurements. The values of  $l$  and  $m$  were 3 and  $-2$  respectively:  $n$  was one of three values;  $+1$ ,  $0$ , or  $-1$ . A single X-band klystron met all the microwave requirements. The  $CO_2$  laser frequency standards were stabilized by the Freed-Javan scheme [14] of locking to the saturation resonance by observing the fluorescence at  $4.3 \mu m$ . The estimated fractional uncertainty in the resetability of our particular

lasers is about  $10^{-9}$  and the absolute frequencies are known to better than one part in  $10^9$  [15, 16]. This permits an uncertainty in the synthesized frequency of about 0.2 MHz.

The particular synthesis scheme selected for each measurement of a CO laser transition was such that the difference between  $\nu_s$  and the CO frequency was less than 1.2 GHz, a frequency dictated by the bandwidth of the spectrum analyzer. When the CO laser radiation was additionally coupled to the MIM diode, a beat note of frequency  $\nu_{B1}$  propagated from the MIM diode, was amplified and displayed on the spectrum analyzer. The CO laser was tuned through its lasing bandwidth and the corresponding excursion of the beat  $\nu_{B1}$  was noted. The center of the excursion was marked by a frequency  $\nu_m$  from the synthesizer, and the CO laser frequency was held at the central frequency during the rest of the measurement. We believe that we can determine the center of the CO transition with a one sigma uncertainty of  $\pm 3$  MHz by this method. This uncertainty did not apply to the frequency of the transfer oscillator, which as we have previously indicated had an uncertainty of about 0.2 MHz.

The basis for the part of the measurement to follow was the frequency

$$\nu_{CO} = \nu_{xfer} = \nu_s + \nu_{B1}. \quad (2)$$

A mirror on a kinematic mount ( $M_1$  in Fig. 1) was removed and the CO laser radiation moved along the indicated path to a HgCdTe mixer where it was combined with the radiation from the TDL.

The TDL portion of the block diagram in Fig. 1 was fairly standard and many details have been described elsewhere [17, 18]. One of the requirements for a successful measurement was a 10 GHz (and preferably smaller) overlap between an  $N_2O$  absorption and a CO laser transition. This was dictated by the HgCdTe detector frequency response. From these possible coincidences, some were discarded because the TDL was not operable at those frequencies. After correct frequency operation was observed and a good mode indicated by fringes produced by the etalon, the monochromator slits were removed. The TDL was frequency modulated and a first derivative lock was used to fix the TDL frequency to that of the  $N_2O$  feature of interest. In cases warranting it, the lock set point was offset from zero to compensate for the background slope of the mode.

At this point, the mirror,  $M_2$ , directing the TDL beam to the etalon was removed and the CO laser-TDL beat note was observed on a second spectrum analyzer. The frequency modulation amplitude was adjusted to the point where no additional broadening

beyond the compressor induced jitter was observed. This was subject to the availability of a signal with good signal-to-noise ratio (SNR) for a suitable lock. The second part of the measurement was a determination of the difference frequency between the transfer oscillator and the frequency locked TDL. This difference frequency beatnote,  $\nu_{B2}$ , was marked by an oscillator whose frequency was counted. The uncertainty in  $\nu_{B2}$  was taken to be one-tenth of the averaged beatnote line width plus one half of the frequency difference between derivative extremes divided by the derivative SNR. As a practical matter, most of the uncertainty came from the beatnote width, since fairly powerful TDLs were used (and consequently a good SNR was the normal case) and the transfer oscillator uncertainty was comparatively small.

The absorption cell used for these measurements was 1.7 m long and pressures of nitrous oxide ranged from 3 to 670 Pa (0.02 to 5 torr). The cell was heated to approximately 150° C for some of the higher  $J$  value transition measurements.

The third item in Fig. 1 was a liquid nitrogen-cooled CO laser. Line selection was afforded by a 180 grooves per mm, high efficiency grating and a compensated zinc selenide mirror with a 10 m radius of curvature was coated to provide 2% output coupling. Additional details of this particular laser may be found in [3].

## Analysis and Fitting of the Measurements

### The Isotopic Bands

The tables of Olson et al. [19] were used to identify the transitions of the  $00^0_1-00^0_0$  bands of  $^{15}N^{14}N^{16}O$  and  $^{14}N^{15}N^{16}O$ . These bands were fit by incorporating the present measurements in a least-squares fit that used the microwave measurements that were compiled by Lovas [11] and infrared measurements taken from Guelachvili [8]. These fits also included the values  $B'$ ,  $B''$ ,  $D'$  and  $D''$  given by Amiot [7] weighted by the uncertainties given by Amiot. Each set of measurements was weighted by the inverse square of its estimated uncertainty. In the fits the infrared measurements that were not based on heterodyne measurements were only used to obtain improved rotational constants, that is to say each set of infrared measurements was allowed to have a different band center. In these fits, the following equations were used for the energy levels:

$$E = G_v + BJ(J+1) - D[J(J+1) - l^2]^2 + H_v[J(J+1) - l^2]^3 + L_v[J(J+1) - l^2]^4 \quad (3)$$

$$\nu_{obs} = E' - E'' \quad (4)$$

**Table 2.** N<sub>2</sub>O rotational constants (in cm<sup>-1</sup>) used in the present analysis

Molecule	State	<i>B</i>	<i>D</i> × 10 <sup>7</sup>	<i>H</i> × 10 <sup>13</sup>
<sup>14</sup> N <sup>15</sup> N <sup>16</sup> O	00 <sup>0</sup> 0	0.418981090(24) <sup>a</sup>	1.762823(505)	2.135(522)
<sup>14</sup> N <sup>15</sup> N <sup>16</sup> O	00 <sup>0</sup> 1	0.417126679(241)	1.754393(2210)	2.485(664)
<sup>15</sup> N <sup>14</sup> N <sup>16</sup> O	00 <sup>0</sup> 0	0.404857271(41)	1.635578(972)	–
<sup>15</sup> N <sup>14</sup> N <sup>16</sup> O	00 <sup>0</sup> 1	0.403262249(136)	1.583169(1128)	–
<sup>14</sup> N <sup>14</sup> N <sup>16</sup> O	00 <sup>0</sup> 0	[0.419010995] <sup>b</sup>	[1.760692]	[–0.17185]
<sup>14</sup> N <sup>14</sup> N <sup>16</sup> O	00 <sup>0</sup> 1 <sup>c</sup>	0.417255087(23)	1.726019(376)	1.247(135)
<sup>14</sup> N <sup>14</sup> N <sup>16</sup> O	00 <sup>0</sup> 2	0.415605328(398)	1.637593(5445)	6.282(956)
<sup>14</sup> N <sup>14</sup> N <sup>16</sup> O	02 <sup>0</sup> 0 <sup>d</sup>	0.419919782(23)	1.869725(393)	–1.531(200)
<sup>14</sup> N <sup>14</sup> N <sup>16</sup> O	02 <sup>2</sup> 0 <sup>d</sup>	0.420124825(18)	1.817141(349)	1.001(244)
<sup>14</sup> N <sup>14</sup> N <sup>16</sup> O	02 <sup>0</sup> 1 <sup>d</sup>	0.418148066(483)	1.89649(232)	–
<sup>14</sup> N <sup>14</sup> N <sup>16</sup> O	02 <sup>2</sup> 1 <sup>d</sup>	0.418529954(764)	1.75418(757)	2.280(2068)

<sup>a</sup> The uncertainty in the last digits (twice the standard error) is given in parentheses

<sup>b</sup> Values in square brackets were taken from [1]

<sup>c</sup> Also included in the fit was  $L = 4.07(149) \times 10^{-18}$  cm<sup>-1</sup>

<sup>d</sup> Other parameters (in cm<sup>-1</sup>) used in the fit were  $L(02^20) = -2.001(406) \times 10^{-17}$ ,  $\delta(02^20-02^00) = 9.612091(49)$ ,  $q(020) = 7.608149(426) \times 10^{-4}$ ,  $q_J(020) = 2.8102(967) \times 10^{-9}$ ,  $q_{JJ}(020) = -4.76(168) \times 10^{-14}$ ,  $q(021) = 8.2508(269) \times 10^{-4}$ , and  $q_J(021) = 3.427(1103) \times 10^{-9}$ ; see (6–10) for the use of these parameters

**Table 3.** Band centers for N<sub>2</sub>O determined by the present heterodyne measurements<sup>a</sup>

Molecule	Vib. transition	$\nu_0$ (cm <sup>-1</sup> )
<sup>14</sup> N <sup>15</sup> N <sup>16</sup> O	00 <sup>0</sup> 1–00 <sup>0</sup> 0	1280.354106(104)
<sup>15</sup> N <sup>14</sup> N <sup>16</sup> O	00 <sup>0</sup> 1–00 <sup>0</sup> 0	1269.892070(66)
<sup>14</sup> N <sup>14</sup> N <sup>16</sup> O	00 <sup>0</sup> 2–00 <sup>0</sup> 1	1278.436094(71)
<sup>14</sup> N <sup>14</sup> N <sup>16</sup> O	00 <sup>0</sup> 2–00 <sup>0</sup> 0	2563.339399(108)
<sup>14</sup> N <sup>14</sup> N <sup>16</sup> O	02 <sup>0</sup> 1–02 <sup>0</sup> 0	1293.863965(107)
<sup>14</sup> N <sup>14</sup> N <sup>16</sup> O	02 <sup>2</sup> 1–02 <sup>2</sup> 0	1297.054025(214)

<sup>a</sup> The uncertainty in the last digits (twice the standard error) is given in parentheses

and

$$\nu_0 = G'_v - G''_v. \quad (5)$$

The rotational constants are given in Table 2, and the band centers ( $\nu_0$ ) are given in Table 3.

### The 00<sup>0</sup>2–00<sup>0</sup>1 Band

To identify the transitions for this band, the transitions were calculated from the constants given by Wells et al. [3] for the lower state and the constants given by Amiot and Guelachvili [6] for the upper state. Improved constants were then obtained by fitting the present measurements and the earlier infrared measurements [3, 5, 6] as well as the microwave measurements [11] for the lower state (the 00<sup>0</sup>1 state). Since the heterodyne frequencies of the N<sub>2</sub>O laser transitions measured by Whitford et al. [5] were also used in this fit, it was necessary to include in the fit the data from [6] and [11] on the upper state of the N<sub>2</sub>O laser transitions. These fits were based

on (3–5) and the resulting constants (pertinent to this paper) are given in Tables 2 and 3. As was done for the isotopic bands just described, the infrared wavelength measurements [6] were only used to help determine the rotational constants whereas the heterodyne measurements were the only measurements used to determine the  $\nu_0$  values given in Table 3.

### The 02<sup>0</sup>1–02<sup>0</sup>0 and 02<sup>2</sup>1–02<sup>2</sup>0 Bands

The transitions for these bands were identified from the calculated tables of transitions that were based on the constants given in [6, 8, 19]. The data were fit by combining the present measurements with the microwave measurements for the two lower states (02<sup>0</sup>0, 02<sup>2</sup>0) given in [11] and with the infrared measurements given in [6, 8, 9, 10, 20, 21] for the states involved in the present measurements. As before, the heterodyne measurements were the only data determining the band centers ( $\nu_0$ 's) given in Table 3.

These bands were originally fit using a modified form of (3–5), but, as shown by Guelachvili [8] and by Toth [10], such a fit tends to require unreasonably large higher order terms in (3) due to the effects of *l*-type resonance between the adjacent *l*=0 and *l*=2 states. Consequently, the constants given in Table 2 and 3 were based on a fit that explicitly allowed for the *l*-type resonance. There is also a significant effect on these transitions due to the well known Fermi resonance between  $\nu_3$  and  $2\nu_2$ , but this resonance was ignored since it was a much smaller effect that could more easily be absorbed into effective constants.

In order to allow for the *l*-type resonance we used the following equations (see [22]) in place of (3):

$$E(02^{2J}0) \text{ or } E(02^{2J}1) = E_A^0 \quad (6)$$

**Table 4.** Wavenumbers calculated for the 00<sup>0</sup>2–00<sup>0</sup>0 Band of N<sub>2</sub>O

P-Branch	J''	R-Branch	P-Branch	J''	R-Branch
–	0	2564.17061( 4) <sup>a</sup>	2530.00461(13)	35	2588.96234(17)
2562.50138( 4)	1	2564.99500( 4)	2528.93317(15)	36	2589.54829(19)
2561.65655( 4)	2	2565.81258( 4)	2527.85528(17)	37	2590.12752(21)
2560.80492( 4)	3	2566.62333( 4)	2526.77098(19)	38	2590.70004(24)
2559.94649( 4)	4	2567.42726( 4)	2525.68027(21)	39	2591.26586(26)
2559.08127( 4)	5	2568.22436( 4)	2524.58317(24)	40	2591.82499(29)
2558.20926( 4)	6	2569.01463( 4)	2523.47971(26)	41	2592.37745(32)
2557.33047( 4)	7	2569.79807( 4)	2522.36991(29)	42	2592.92325(35)
2556.44490( 4)	8	2570.57467( 4)	2521.25378(32)	43	2593.46240(37)
2555.55257( 4)	9	2571.34444( 4)	2520.13136(35)	44	2593.99493(39)
2554.65347( 4)	10	2572.10737( 4)	2519.00265(37)	45	2594.52085(43)
2553.74762( 4)	11	2572.86346( 4)	2517.86770(39)	46	2595.04016(46)
2552.83502( 4)	12	2573.61272( 4)	2516.72652(43)	47	2595.55290(49)
2551.91568( 4)	13	2574.35513( 4)	2515.57913(46)	48	2596.05909(52)
2550.98960( 4)	14	2575.09071( 4)	2514.42557(49)	49	2596.55872(54)
2550.05680( 4)	15	2575.81945( 4)	2513.26586(52)	50	2597.05184(58)
2549.11729( 4)	16	2576.54135( 4)	2512.10003(54)	51	2597.53847(60)
2548.17107( 4)	17	2577.25641( 4)	2510.92810(58)	52	2598.01861(62)
2547.21815( 4)	18	2577.96465( 4)	2509.75012(60)	53	2598.49230(65)
2546.25854( 4)	19	2578.66604( 4)	2508.56610(62)	54	2598.95956(67)
2545.29225( 4)	20	2579.36061( 4)	2507.37607(65)	55	2599.42041(68)
2544.31930( 4)	21	2580.04835( 4)	2506.18008(67)	56	2599.87488(69)
2543.33969( 4)	22	2580.72927( 6)	2504.97815(68)	57	2600.32301(69)
2542.35343( 4)	23	2581.40336( 6)	2503.77033(69)	58	2600.76480(69)
2541.36054( 6)	24	2582.07064( 6)	2502.55663(69)	59	2601.20030(68)
2540.36103( 6)	25	2582.73110( 6)	2501.33711(69)	60	2601.62954(67)
2539.35490( 6)	26	2583.38476( 6)	2500.11179(68)	61	2602.05254(64)
2538.34218( 6)	27	2584.03161( 7)	2498.88072(67)	62	2602.46934(61)
2537.32288( 6)	28	2584.67167( 7)	2497.64394(64)	63	2602.87998(57)
2536.29700( 7)	29	2585.30494( 8)	2496.40149(61)	64	2603.28448(52)
2535.26457( 7)	30	2585.93142( 8)	2495.15340(57)	65	2603.68288(45)
2534.22560( 8)	31	2586.55112( 9)	2493.89973(52)	66	2604.07522(38)
2533.18010( 8)	32	2587.16406(12)	2492.64052(45)	67	2604.46155(30)
2532.12809( 9)	33	2587.77024(13)	2491.37581(38)	68	2604.84189(24)
2531.06959(12)	34	2588.36966(15)	2490.10566(31)	69	2605.21630(21)

<sup>a</sup> The uncertainty in the last digits (one standard error) is given in parentheses

$$\begin{aligned}
 E(02^00) \text{ or } E(02^01) &= E_{\Sigma} \\
 &= E_{\Sigma}^0 + 1/2\delta - 1/2\{\delta^2 + 4q^2[J^2(J+1)^2 \\
 &\quad - 2J(J+1)]\}^{1/2},
 \end{aligned} \tag{7}$$

and

$$\begin{aligned}
 E(02^{2e}0) \text{ or } E(02^{2e}1) &= E_{\Delta} \\
 &= E_{\Delta}^0 - 1/2\delta + 1/2\{\delta^2 + 4q^2[J^2(J+1)^2 \\
 &\quad - 2J(J+1)]\}^{1/2},
 \end{aligned} \tag{8}$$

where  $E_{\Sigma}^0$  and  $E_{\Delta}^0$  are given by (3), with  $l=0$  and 2 respectively,

$$\delta = E_{\Delta}^0 - E_{\Sigma}^0, \tag{9}$$

and

$$q = q_v - q_{vJ}J(J+1) + q_{vJJ}J^2(J+1)^2. \tag{10}$$

Since the transitions, as defined by these equations, are a nonlinear function of the various constants, the measurements were fit by means of a nonlinear least-squares program which was written to handle the fitting of transitions involving  $l$ -type resonance.

One of the parameters governing the  $l$ -type resonance is the energy difference  $\delta(02^{20}-02^00)$  for which the present measurements do not provide any direct information. To provide a direct measure of  $\delta(02^{20}-02^00)$  and to help fix the rotational constants for the lower vibrational levels ( $02^{20}$  and  $02^00$ ), we have included in the least-squares fit the data for the transitions  $02^{20}-01^10$  and  $02^00-01^10$  given by Kauppinen [21] and the data for the transitions  $02^{20}-00^00$  and  $02^00-00^00$  given by Toth [10].

The reader is cautioned to remember that all the constants given in Tables 2 and 3 (including those

in the footnotes) and required by (6–10) must be used in order to calculate the transitions or energy levels for the  $02^01$ ,  $02^21$ ,  $02^00$ , and  $02^20$  states. The present method of fitting these levels is particularly useful for interpolation or for extrapolation since it eliminates the unreasonably large values for the higher order constants otherwise required by (3) when the  $l$ -type resonance is ignored. This method of fitting the data allowed us to fit the microwave measurements for the  $02^00$  and  $02^20$  states to within experimental error (better than  $\pm 0.01$  MHz for the most accurate  $J \geq 14$  transitions). Toth [10] was only able to fit the microwave measurements to about  $\pm 0.15$  MHz.

### The $03^11$ – $03^10$ and $03^31$ – $03^30$ Bands

The other transitions identified in Table 1 do not give the requisite number of independent measurements of these bands to provide a reasonable basis for a least-squares fit. Consequently, we present these measurements, but have not attempted to use them to improve the constants for the levels involved. The assignment of the one  $03^31$ – $03^30$  transition is based largely on a process of elimination since we know of no other observations of the two levels involved. More transitions would have to be observed to verify this assignment.

### Discussion

The present measurements of the  $00^01$ – $00^00$  transitions of  $^{15}\text{N}^{14}\text{N}^{16}\text{O}$  and  $^{14}\text{N}^{15}\text{N}^{16}\text{O}$  can be compared with the measurements of Guelachvili [8] who obtained band centers that were higher by 7.2 MHz and 8.7 MHz respectively. Our earlier measurements on the  $00^01$ – $00^00$  and  $01^11$ – $01^10$  transitions of  $^{14}\text{N}^{14}\text{N}^{16}\text{O}$  were also lower than those of Guelachvili as were the measurements of Brown and Toth [9].

By combining the present constants for the  $00^02$ – $00^01$  band with the earlier constants determined for the  $00^01$ – $00^00$  band [3], we have calculated the transition frequencies and their uncertainties for the  $00^02$ – $00^00$  band near  $2560\text{ cm}^{-1}$  as given in Table 4. The present wavenumbers are within  $0.001\text{ cm}^{-1}$  of the values given in Table 7 of Ref. [6].

The present  $02^01$ – $02^00$  band measurements could also be combined with measurements on the  $02^00$ – $00^00$  band to give frequency values for the  $02^01$ – $00^00$  transitions near  $2460\text{ cm}^{-1}$ . Although Wells et al. [2] measured one high- $J$  transition for the  $02^00$ – $00^00$  band, that was not sufficient to give reliable values for the  $02^01$ – $00^00$  transitions and more extensive direct heterodyne measurements are not possible at this time. A more promising direction for

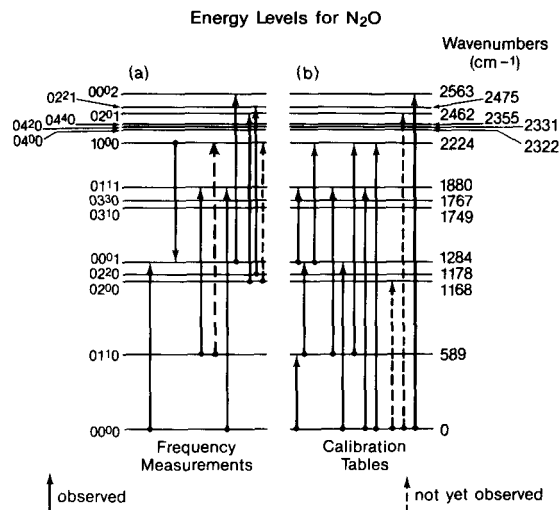


Fig. 2. Energy level diagram that indicates on the left (a) frequency measurements made to date on  $\text{N}_2\text{O}$  (solid arrows), or those where measurements will be made (dashed arrows). Note that  $\nu_1$  and  $\nu_3$  are interchanged from notation used by some authors. On the right (b) are arrows representing calibration tables prepared from constants determined by the measurements

heterodyne measurements on the  $02^00$  level would be to measure the very weak  $10^00$ – $02^00$  band at  $1056\text{ cm}^{-1}$  (see Fig. 2). Alternatively the very good wavelength measurements of Toth [10] and of Brown and Toth [9] for the  $02^00$ – $00^00$  band could be used.

Frequency measurements to date (present work and those in [2, 3, 5]) on the lowest levels of  $\text{N}_2\text{O}$  are summarized in Fig. 2. As mentioned previously, the energy levels are labelled according to the IAU-IUPAP recommendations [4]. Also indicated in Fig. 2 are transitions representing bands whose frequencies have been calculated for calibration purposes. An interim  $\text{N}_2\text{O}$  calibration atlas is most readily obtained by contacting either of the NBS authors.

We would like to thank Robert Toth (JPL) for sending us a preprint of his latest FTS measurements of this same band system [10]; also we thank J. Kauppinen (Oulu, Finland) for sending us the latest results of his FTS measurements of hot bands in the  $\nu_2$  region [21]. One of us (A.H.) would like to thank the Time and Frequency Division for the warm hospitality extended by the NBS during this collaboration. We thank our colleague, D.A. Jennings, for the use of his computer programs for the frequency synthesis operation. The continuing fine work on our manuscripts by our editorial assistant, G. Bennett, is also much appreciated. We extend our gratitude for partial support of this work to the NASA Office of Upper Atmospheric Research.

### References

1. Pollock, C.R., Petersen, F.R., Jennings, D.A., Wells, J.S., Maki, A.G.: *J. Mol. Spectrosc.* **107**, 62 (1984)
2. Wells, J.S., Jennings, D.A., Hinz, A., Murray, J.S., Maki, A.G.: *J. Opt. Soc. Am.* **B2**, 857 (1985)

3. Wells, J.S., Hinz, A., Maki, A.G.: *J. Mol. Spectrosc.* **114**, 84 (1985)
4. Mulliken, R.S.: *J. Chem. Phys.* **23**, 1997 (1955)
5. Whitford, B.G., Siemsen, K.J., Riccius, H.D., Hanes, G.R.: *Opt. Comm.* **14**, 70 (1975)
6. Amiot, C., Guelachvili, G.: *J. Mol. Spectrosc.* **59**, 171 (1976); also private communication, Amiot and Guelachvili, Laboratoire d'Infrarouge, Orsay, France
7. Amiot, C.: *J. Mol. Spectrosc.* **59**, 191 (1976)
8. Guelachvili, G.: *Can. J. Phys.* **60**, 1334 (1982)
9. Brown, L.R., Toth, R.A.: *J. Opt. Soc. Am.* **B2**, 842 (1985)
10. Toth, R.A.: *J. Opt. Soc. Am.* **B3**, 1263 (1986)
11. Lovas, F.J.: *J. Phys. Chem. Ref. Data* **7**, 1445 (1978)
12. Guelachvili, G., de Villeneuve, D., Farrenq, R., Urban, W., Verges, J.: *J. Mol. Spectrosc.* **98**, 64 (1983)
13. Dale, R.M., Herman, M., Johns, J.W.C., McKellar, A.R.W., Nagler, S., Strathy, I.K.M.: *Can. J. Phys.* **57**, 677 (1979)
14. Freed, C., Javan, A.: *Appl. Phys. Lett.* **17**, 53 (1970)
15. Petersen, F.R., Beaty, E.C., Pollock, C.R.: *J. Mol. Spectrosc.* **102**, 112 (1983)
16. Bradley, L.C., Soohoo, K.L., Freed, C.: *IEEE J. Quantum Electron.* **QE-22**, 234 (1986)
17. Wells, J.S., Jennings, D.A., Maki, A.G.: *J. Mol. Spectrosc.* **107**, 48 (1984)
18. Wells, J.S., Petersen, F.R., Maki, A.G.: *Appl. Opt.* **18**, 3567 (1979)
19. Olson, W.B., Maki, A.G., Lafferty, W.J.: *J. Phys. Chem. Ref. Data* **10**, 1065 (1981)
20. Jolma, K., Kauppinen, J., Horneman, V.-M.: *J. Mol. Spectrosc.* **101**, 278 (1983)
21. J. Kauppinen: Private Communication
22. Maki, A.G., Lide, D.R.: *J. Chem. Phys.* **47**, 3206 (1967)
23. Brown, J.M., Hougen, J.T., Huber, K.-P., Johns, J.W.C., Kopp, I., Lefebvre-Brion, H., Merer, A.J., Ramsay, D.A., Rostas, J., Zare, R.N.: *J. Mol. Spectrosc.* **55**, 500 (1975)

A. Hinz  
Institut für Angewandte Physik  
der Universität Bonn  
Wegelerstrasse 8  
D-5300 Bonn  
Federal Republic of Germany

J.S. Wells  
Time and Frequency Division  
National Bureau of Standards  
Boulder, CO 80303  
USA

A.G. Maki  
Molecular Spectroscopy Division  
National Bureau of Standards  
Gaithersburg, MD 20899  
USA